Euclidean resonance in a magnetic field

B. Ivlev
Department of Physics and Astronomy and NanoCenter, University of South Carolina, Columbia, South Carolina 29208, USA and Instituto de Física, Universidad Autónoma de San Luis Potosí, San Luis Potosí, San Luis Potosí, 78000 Mexico
(Received 18 May 2007; revised manuscript received 15 June 2007; published 28 August 2007)

An analogy is found between Wigner resonant tunneling and tunneling across a static potential barrier in a static magnetic field. Whereas in the process of Wigner tunneling an electron encounters a classically allowed region where a discrete energy level coincides with its energy, in the magnetic field the potential barrier is constant in the direction of tunneling. Along the tunneling path, certain regions are formed where, in the classical language, the kinetic energy of the motion perpendicular to tunneling is negative. These regions play the role of potential wells, where a discrete energy level can coincide with the electron energy. This phenomenon, which occurs at a certain magnetic field, is called Euclidean resonance and substantially depends on the shape of the potential forces in the direction perpendicular to tunneling. Under conditions of Euclidean resonance, a long-distance underbarrier motion is possible, which can be observed in experiments.

DOI: 10.1103/PhysRevA.76.022108 PACS number(s): 03.65.Xp, 03.65.Sq

I. INTRODUCTION

It is known that long-distance motion under a classical static potential barrier is impossible except for a short WKB penetration [1]. This is true in the one-dimensional case. In two dimensions x and y, the situation can be more complicated. When, in addition, a magnetic field is applied along the z axis the scenario under the barrier, where classical motion is impossible, may become very peculiar. If the barrier, described by a potential energy $V(x,y)$, is flat, the wave function decays in the x direction in the classically forbidden region as $\psi \sim \exp(-c_1 x^2/l^2)$ where $l=\sqrt{\hbar/m\omega_c}$ is the magnetic length, $\omega_c=|e|H/mc$ is the cyclotron frequency, and c_1 is a numerical constant [1]. This result is true when x exceeds the cyclotron radius.

The underbarrier decay of the wave function becomes substantially different when the potential barrier is not a constant in the (x,y) plane, with a typical spatial scale a [2–6]. In this case, when the cyclotron length is shorter than a, the wave function decays more slowly, as $\psi \sim \exp(-c_2 a x/l^2)$. This result looks unusual since it is valid even when the nonhomogeneous barrier is higher at each point than the flat one. In other words, a higher potential barrier is more transparent, which is counterintuitive from the standpoint of WKB theory.

Even more counterintuitive physics is related to a lower magnetic field, when the cyclotron radius is of the order of a [7]. In this case, when the magnetic field is close to a certain value H_R, decay of the wave function under the barrier can be nonexponential in space. This means a long-range penetration of a particle under an almost classical potential barrier. This phenomenon is called Euclidean resonance.

In [7] Euclidean resonance was investigated on the basis of classical underbarrier trajectories in imaginary time. This method allowed the phenomenon to be established, but its characteristics important for experimental observation remained in shadow. The main characteristic is the coordinate dependence of the wave function under the barrier.

This paper is focused on two aspects. First, the coordinate dependence of the wave function is found here. At a small magnetic field, the underbarrier wave function decays almost according to WKB theory. It has only small periodically distributed peaks. At a higher magnetic field, those peaks increase, giving rise to strong oscillations of the wave function under the barrier. There is a certain field H_0, such that at $H > H_0$ the main peak in the electron density is located at a finite distance inside the barrier. When the magnetic field approaches the resonance value $H_R > H_0$, the periodically distributed underbarrier peaks have almost the same amplitude. Their amplitudes decrease inside the barrier but not exponentially with distance. This means that the particle can penetrate over a long distance under the classical barrier. We emphasize that the particle energy is strictly below the potential barrier at each point. A possible experimental situation is described in Sec. X.

Second, in this paper an interpretation of Euclidean resonance in a magnetic field is proposed. A topological vortex state under the barrier is formed, which results in an effective potential well. Euclidean resonance corresponds to coincidence of a level in that well with the electron energy.

Euclidean resonance (formation of long-range coherence) constitutes a phenomenon that can be considered as the opposite pole with respect to Anderson localization (destruction of the long-range coherence) [8].

Tunneling in a magnetic field was addressed in Refs. [2–7,9–14]. The physical part of the paper relates to Secs. II and IX–XI. The mathematical part is presented in Secs. III–VIII.

II. GENERAL ARGUMENTS

In this section we consider some general properties of an underbarrier motion in a magnetic field. In the classical language, besides a kinetic energy in the direction of tunneling, there is also a transverse kinetic energy (in the perpendicular direction). In terms of the Schrödinger equation, those parts are proportional to second derivatives of the wave function. An underbarrier propagating motion, in principle, is possible if the transverse kinetic energy is negative, in order to com-

pensate the total negative energy, allowing a positive kinetic energy in the direction of tunneling.

Let us specify the problem in more detail. Suppose that the tunneling path is in the x direction, and away from the ends of the path the total potential energy is $u(y)$. This function is even and has the minimum $u(0)=0$. The magnetic field is directed along the z axis. So the negative electron energy E corresponds to an underbarrier motion. One can write down the effective Schrödinger equation for motion in the x direction for the wave function $\varphi(x)=\psi(x,0)$,

$$-\frac{\hbar^2}{2m}\frac{\partial^2\varphi(x)}{\partial x^2}+U(x)\varphi=E\varphi, \tag{1}$$

where $U(x)=-(\hbar^2/2m\psi)\partial^2\psi/\partial y^2$ is taken at $y=0$. We use the gauge $\vec{A}=\{-Hy,0,0\}$. The wave function can be expressed through the modulus and the phase as $\psi=|\psi|\exp(i\chi)$. Since the potential $u(y)$ is symmetric, the modulus of the wave function is even and the phase χ is odd with respect to y. For this reason, the effective potential

$$U(x)=\frac{\hbar^2}{2m}\left[\left(\frac{\partial\chi}{\partial y}\right)^2-\frac{1}{|\psi|}\frac{\partial^2|\psi|}{\partial y^2}\right]_{y=0} \tag{2}$$

is real.

In the absence of the magnetic field there is nothing surprising. An electron is localized at the center of the potential $u(y)$, at $y=0$, where $|\psi|$ has a maximum. Therefore, both terms in Eq. (2) are positive. In this case, $U(x)$ is positive and the underbarrier motion with total negative energy E relates to an exponential decay of the wave function of the WKB type.

In a magnetic field the situation can be substantially different. Although the minimum of the potential energy $u(y)$ is at $y=0$, due to Lorentz forces, the maxima of the electron distribution can be shifted symmetrically away from the line $y=0$ (disjoining effect). In this case $\partial^2|\psi|/\partial y^2$ is positive at $y=0$, and the second term in Eq. (2) is negative. Such a disjoining electron distribution was pointed out in Refs. [10,7]. We discuss the disjoining effect below.

It is hard to conclude in advance that the disjoining distribution of the electron density away from the center, $y=0$, [the second term in Eq. (2)] is sufficient to drive the total $U(x)$ to a negative value. Nevertheless, on the basis of the analytical solution of Ref. [7], it is found that the potential $U(x)$ has the form of negative potential wells. One can compare the positions of discrete energy levels in those wells with the value of the electron energy $E<0$ according to Eq. (1). If, under variation of the magnetic field, some level in the well $U(x)$ approaches the energy E, this should result in the resonance phenomenon called Euclidean resonance [7].

Euclidean resonance in a magnetic field recalls the phenomenon of Wigner resonant tunneling [1], when in the middle of a potential barrier there is a well with a level close to the particle energy. But an essential difference is that in Euclidean resonance the initial system is homogeneous along the direction of tunneling and the effective wells are formed by an intrinsic mechanism due to transverse motion.

When the negative underbarrier energy E is fixed, one can compare it with the energy parameter $m\omega_c^2a^2$, where a is the typical spatial scale of the potential $u(y)$. In the limit of high magnetic fields, $m\omega_c^2a^2\gg|E|$, energy levels in the potential well $U(x)$ are of the order of $-m\omega_c^2a^2$, which is substantially lower than the energy E. In this case there is no level coincidence.

Upon reduction of the magnetic field, the two energies become of the same order of magnitude, $-m\omega_c^2a^2\sim E$, which indicates the possibility in principle of level coincidence. As calculations show, this occurs at the magnetic field H_R, which can be called the resonance magnetic field. The analytical form of the potential $u(y)$ in the plane of complex y plays a crucial role. For example, Euclidean resonance is absent for a pure quadratic $u(y)$. This sensitivity is a consequence of interference of underbarrier cyclotron paths that are reflected from the potential $u(y)$.

Near the resonance field H_R, the underbarrier exponential decay of the wave function becomes weak due to the resonant connection of different potential wells. At $H=H_R$ there is no exponential decay (perhaps a power law). In the following sections we consider this problem in detail.

III. FORMULATION OF THE PROBLEM

We consider an eigenstate with a negative energy E_1 of the Schrödinger equation

$$-\frac{\hbar^2}{2m}\left(\frac{\partial}{\partial x}-\frac{iy}{l^2}\right)^2\psi-\frac{\hbar^2}{2m}\frac{\partial^2\psi}{\partial y^2}+[V(x)+u(y)]\psi=E_1\psi \tag{3}$$

in a magnetic field directed along the z axis. The x part of the potential is the negative δ well $V(x)=-\hbar\sqrt{2|E|/m}\delta(x)$. The y part has the form

$$u(y)=u_0\left(\frac{y}{a}\right)^{4N}, \tag{4}$$

where N is a large integer number. The potential (4) represents approximately two infinite potential walls at the points $y=\pm a$. In the absence of a magnetic field the lower discrete energy level in the potential $u(y)$ can be estimated as $\hbar^2/ma^2$. The energies $|E|$ and $\hbar\omega_c$ are supposed to be large compared to that energy

$$\frac{\hbar^2}{ma^2}\ll|E|,\quad l\ll a. \tag{5}$$

The second condition (5) can also be expressed in the form $1\ll n$, where

$$n=\frac{Ha^2}{\Phi_0} \tag{6}$$

is the number of flux quanta $\Phi_0=\pi c\hbar/|e|$ of the total magnetic flux through the area a^2.

The boundary condition for the region $x>0$ has the form

$$\hbar\left(\frac{\partial}{\partial x}-\frac{iy}{l^2}\right)\psi(x,y)\Big|_{x=0}=-\sqrt{2m|E|}\psi(0,y). \tag{7}$$

Under the semiclassical conditions (5) the eigenvalue E_1 almost coincides with E.

IV. THE HAMILTON-JACOBI EQUATION

One can always specify the wave function in the form

$$\psi(x,y) = \exp\left(\frac{iS(x,y)}{\hbar}\right), \tag{8}$$

where $S(x,y)$ satisfies the equation

$$\frac{1}{2m}\left(\frac{\partial S}{\partial x} - m\omega_c y\right)^2 + \frac{1}{2m}\left(\frac{\partial S}{\partial y}\right)^2 - \frac{i\hbar}{2m}\nabla^2 S = E. \tag{9}$$

The boundary condition (7) is now transformed into

$$\left.\frac{\partial S(x,y)}{\partial x}\right|_{x=0} = i\sqrt{2m|E|} + m\omega_c y. \tag{10}$$

Below we measure x and y in units of the cyclotron length

$$L = \sqrt{\frac{2|E|}{m\omega_c^2}} = l\sqrt{\frac{2|E|}{\hbar\omega_c}}. \tag{11}$$

The new function $\sigma(x,y)$ is introduced,

$$S(x,y) = i\frac{2|E|}{\omega_c}\sigma(x,y), \tag{12}$$

which obeys the equation

$$\left(\frac{\partial\sigma}{\partial x} + iy\right)^2 + \left(\frac{\partial\sigma}{\partial y}\right)^2 - \frac{\hbar\omega_c}{2|E|}\left(\frac{\partial^2\sigma}{\partial x^2} + \frac{\partial^2\sigma}{\partial y^2}\right) = 1 \tag{13}$$

with the boundary condition

$$\left.\frac{\partial\sigma(x,y)}{\partial x}\right|_{x=0} = 1 - iy. \tag{14}$$

Reflection occurs at the points $y = \pm\alpha$, where

$$\alpha = \sqrt{\frac{m\omega_c^2 a^2}{2|E|}} = \frac{a}{L}. \tag{15}$$

We consider below the limit of a relatively small magnetic field $\hbar\omega_c \ll |E|$. In this case one can write Eq. (13) in the form of the Hamilton-Jacobi equation

$$\left(\frac{\partial\sigma}{\partial x} + iy\right)^2 + \left(\frac{\partial\sigma}{\partial y}\right)^2 = 1, \tag{16}$$

where σ plays the role of a classical action.

V. SOLUTION OF THE HAMILTON-JACOBI EQUATION

Equation (16) can be solved by the variation of constants as described in [15]. The general integral of the Hamilton-Jacobi equation has the form

$$\sigma(x,y) = vx + \int_0^y dy_1\sqrt{1 + (y_1 - iv)^2} + F(v), \tag{17}$$

where a certain function $v(x,y)$ is introduced which should be determined from the condition (independence of σ on v)

$$x - i\int_0^y \frac{(y_1 - iv)dy_1}{\sqrt{1 + (y_1 - iv)^2}} + \frac{\partial F(v)}{\partial v} = 0. \tag{18}$$

According to that, the following relations hold:

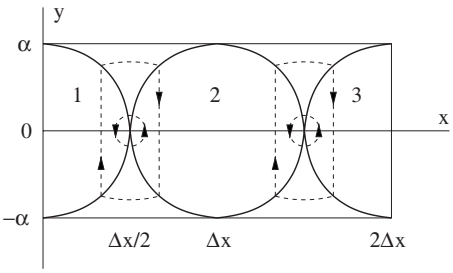

FIG. 1. Reflection-induced curves restrict the regions 1, 2, and 3, where the reflectionless approximation holds. The dashed paths show the electric current of vortices.

$$\frac{\partial\sigma(x,y)}{\partial x} = v(x,y), \quad \frac{\partial\sigma(x,y)}{\partial y} = \sqrt{1 + [y - iv(x,y)]^2}. \tag{19}$$

The function $F(v)$ should be determined from the condition (14), which now reads

$$v(0,y) = 1 - iy. \tag{20}$$

If we express y through $v(0,y)$ and insert it into Eq. (18) at $x=0$, we obtain the functional dependence

$$\frac{\partial F(v)}{\partial v} = \sqrt{v^2 - 1}. \tag{21}$$

Equation (18), which determines the function $v(x,y)$, takes the form

$$x = i\int_{iv-i}^{y} \frac{(y_1 - iv)dy_1}{\sqrt{1 + (y_1 - iv)^2}}. \tag{22}$$

As follows from Eq. (22), $v(x,y) = \sqrt{1+x^2} - iy$. With this definition, Eq. (19) yields

$$\frac{\partial\sigma(x,y)}{\partial x} = \sqrt{1 + x^2} - iy, \quad \frac{\partial\sigma(x,y)}{\partial y} = ix. \tag{23}$$

The form (17) and Eqs. (21)–(23) hold at a certain part of the (x,y) plane. The integration variable y_1 in Eq. (22) varies between the limits y and $i(\sqrt{1+x^2}-1)+y$. Our reflectionless approach $[u(y) \simeq 0]$ is valid when $|y_1| < \alpha$. This condition reads

$$(\sqrt{1 + x^2} - 1)^2 + y^2 < \alpha^2. \tag{24}$$

The condition (24) defines the area in the (x,y) plane, marked as 1 in Fig. 1. The area 1 is restricted by the solid curve, which can be treated as reflection-induced. This means that it accumulates interfering waves reflected from the walls. The period of the structure is $\Delta x = 2\sqrt{\alpha(2+\alpha)}$. In physical units

$$\Delta x = 2a\left(1 + \sqrt{\frac{8|E|}{m\omega_c^2 a^2}}\right)^{1/2}. \tag{25}$$

According to Eqs. (8), (12), and (23), at $0 < x < \Delta x/2$, in physical units,

$$|\psi(x,0)| \sim \exp\left\{-\frac{|E|}{\hbar\omega_c}\left[\frac{x}{L}\sqrt{1+\frac{x^2}{L^2}}+\ln\left(\frac{x}{L}+\sqrt{1+\frac{x^2}{L^2}}\right)\right]\right\}. \tag{26}$$

At a distance δ around the point $x=\Delta x/2$, $y=0$, the semiclassical approximation breaks down. The scale δ can be estimated from Eq. (13). The two terms p_x^2 and $(\hbar\omega_c/|E|)\partial p_x/\partial x$, where $p_x=\partial\sigma/\partial x$, should be of the same order of magnitude within the nonsemiclassical region. In physical units this gives the estimate $\delta\sim l^2/a$. There is a clear interpretation of the quantum length δ. The cyclotron length (11) is estimated as $L\sim p/m\omega_c$. The length δ can be obtained from the same relation if we set $L\sim a$ and use the quantum uncertainty condition $p\sim\hbar/\delta$. The length δ has the meaning of a quantum uncertainty in the position of the center of a cyclotron orbit (Lorentz drift uncertainty).

How can we go beyond the region 1 in Fig. 1? In the semiclassical problem of a one-dimensional overbarrier motion, there is an effect of formation of a reflected wave at a certain point x (Stokes phenomenon). At this point the Stokes line, which starts at the complex point x_R, intersects the real axis [16]. The easiest way to obtain the reflected wave is to go in the complex plane up to x_R, where the two branches (incident and reflected) merge, and to return to the real axis. This method accounts for the delicate interference of partial de Broglie waves emitted by the particle.

In our problem the situation is qualitatively similar. The two branches, related to the regions 1 and 2 in Fig. 1, also merge at a certain complex point $x=\Delta x/2$, $y=-i\eta$. At that point the root in Eq. (19) becomes zero if we take account into the entire potential (4). The solution, generated in this way in the region 2, is $\sigma_2(x,y)=\sigma(x-\Delta x,y)+\text{const}$. The constant can be determined by the same method of going in to the complex plane of the variables. This program is performed in the next section.

VI. CLASSICAL TRAJECTORIES

The classical path from the region 1 to the region 2 in Fig. 1 goes through the complex plane of coordinates between the physical points $\{x=0,\ y=0\}$ and $\{x=\Delta x,\ y=0\}$. Along this path, x is real but $y=-i\eta$ is imaginary. This path corresponds to a trajectory in imaginary time $t=-i\tau$. The proper formalism is developed in Ref. [7] and results in

$$\left|\frac{\psi(\Delta x,0)}{\psi(0,0)}\right|^2 \sim \exp(-A), \tag{27}$$

where

$$A = A_{WKB}(\Delta x) - \frac{2m}{\hbar}\int d\tau\left(\frac{\partial\eta}{\partial\tau}\right)^2. \tag{28}$$

The integral in Eq. (28) is taken along one period of the periodic motion described by the classical equation

$$\frac{m}{2}\left(\frac{\partial\eta}{\partial\tau}\right)^2 - \frac{m\omega_c^2}{2}(\eta+L)^2 + u(-i\eta) = E. \tag{29}$$

The last term in Eq. (28) reduces the total action and can be interpreted as originating from the transverse kinetic energy

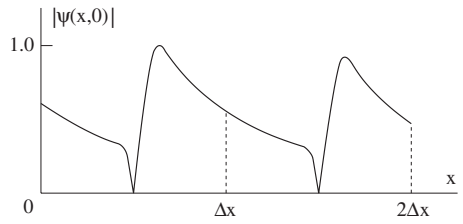

FIG. 2. Modulus of the wave function decays slightly, when H is close to H_R. The long-range semiclassical parts are connected by short vortex regions, of width l^2/a, localized near the points $x=\Delta x/2$ and $3\Delta x/2$, where $\psi=0$.

as discussed in Sec. I. The action (28) has the form

$$A = \left(1 - \int_0^\alpha d\eta\sqrt{\frac{\eta(2+\eta)}{\alpha(2+\alpha)}}\right)A_{WKB}(\Delta x), \tag{30}$$

where the WKB action is $A_{WKB}(\Delta x)=2\Delta x\sqrt{2m|E|}/\hbar$. The wave function in the region 1 in Fig. 1 is given by Eqs. (8), (12), (17), (21), and (22). In the region 2 the action $\sigma_2(x,y)$ is expressed through the function $\sigma(x,y)$ by the equation

$$\sigma_2(x,y) - \sigma(x-\Delta x,y) = \Delta x - 2\int_0^\alpha d\eta\sqrt{(\eta+1)^2-1}. \tag{31}$$

The same relation holds for the region 3 in Fig. 1, namely, the difference $\sigma_3(x,y)-\sigma_2(x-\Delta x,y)$ coincides with the right-hand side of Eq. (31).

The function $|\psi(x,y)|$ does not depend on y in the regions 1, 2, and 3. The modulus $|\psi(x,0)|$ is plotted schematically in Fig. 2. The vortex cores are located at the points $x=\Delta x/2$ and $x=3\Delta x/2$, where $\psi=0$ [1]. This is analogous to Fig. 3.

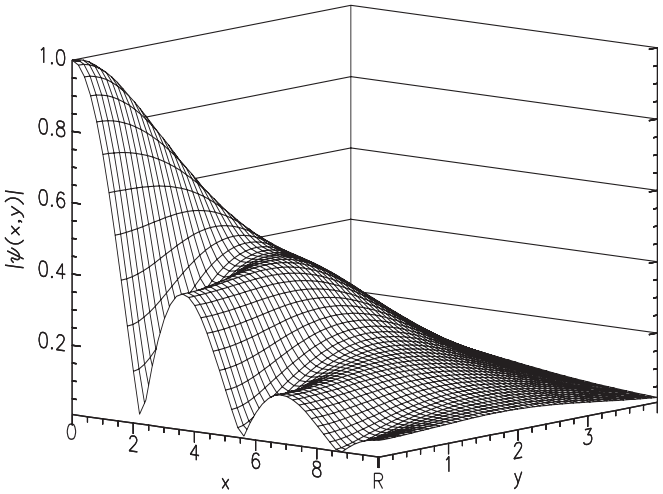

FIG. 3. Modulus of the wave function from Ref. [7], when the magnetic field is high, $m\omega_c^2a^2\gg|E|$. The plot is symmetric with respect to the line $y=0$. The variables x and y are measured in units of $2l^2/a$.

Under an increase of the magnetic field, the parameter α increases and, when it reaches the value $\alpha_R \simeq 1.66$, the right-hand sides of Eqs. (30) and (31) formally become zero. This occurs at the resonance magnetic field

$$H_R = \frac{c\sqrt{2m|E|}}{|e|a}\alpha_R. \tag{32}$$

One can simply show that, close to H_R,

$$\left|\frac{\psi(R,0)}{\psi(0,0)}\right|^2 \sim \exp\left(-0.94\frac{H_R - H}{H_R}A_{WKB}(R)\right), \tag{33}$$

where R is an integer multiple of Δx. Under the resonance condition $H=H_R$, the spatial scale in Figs. 1 and 2 is $\Delta x \simeq 2.97a$. Our semiclassical method is applicable when the action is formally large. So there is a restriction $1/A_{WKB} \ll (H_R-H)/H_R \ll 1$. To really approach the resonance field H_R one should go beyond the semiclassical approximation.

VII. ELECTRIC CURRENT UNDER THE BARRIER

The electric current $\vec{j}=-e^2|\psi|^2\vec{Q}/mc$ is expressed through the gauge-invariant vector potential $\vec{Q}=\vec{A}+Hl^2\nabla\chi$, which depends on the phase $\chi=-2|E|\mathrm{Im}\,\sigma/\hbar\omega_c$ of the wave function $\psi=|\psi|\exp(i\chi)$ [1]. With the gauge $\vec{A}=\{-Hy,0,0\}$ used, there is only a y component of $\vec{Q}$ in the regions 1, $-Hx$, and 2, $-H(x-\Delta x)$. The electric current distribution is shown by the dashed curves in Fig. 1.

There are topological vortices at the points $\{\Delta x/2,0\}$ and $\{3\Delta x/2,0\}$, as in Fig. 3. The vorticity along the dashed small loop, of size δ, in Fig. 1,

$$\oint \vec{Q}\,d\vec{l} = -2\Phi_0, \tag{34}$$

is determined by the topological properties [17]. The vorticity along the large dashed loop, of size a, changes sign in order to provide the total positive magnetic flux

$$\Phi = 2\Phi_0 + \oint \vec{Q}\,d\vec{l} \tag{35}$$

through the area restricted by the large loop. In Eqs. (34) and (35), the contours of integration are counterclockwise. In contrast to vortices in superconductors, in this case there is no Meissner screening, which would cancel the second term in Eq. (35) at a large distance, resulting in quantization of flux [17]. One should emphasize the opposite roles of different parts of the vortices. At the outer part of the vortex (the large dashed loop in Fig. 1) the Lorentz force is directed inside the loop, leading to joining of the electron density to the vicinity of the vortex. This results in the peaks of $|\psi|$ in Fig. 2. At the inner part (the small dashed loop) the Lorentz force is directed outside the loop, leading to the local disjoining of the electron density in close vicinity to the vortex topological point ($\psi=0$) in Fig. 2.

The current paths are continued outside the regions 1, 2, and 3 in Fig. 1, where we do not know the detailed form of the wave function. The vortex structure of the wave function is the consequence of the specific analytical form of the potential $u(y)$ [7] and does not depend on the magnetic field. For example, for a quadratic $u(y)$, topological vortices under the barrier are absent and there are smooth current curves only.

VIII. CHOICE OF $u(y)$

We use the potential $u(y)$ determined by Eq. (4) with a large N, which allows us to treat the potential (4) as infinite walls at $y=\pm a$ and $y=\pm ia$. For the semiclassical approach, N should not be too large. The typical scale near the wall, $\delta y \sim a/N$, has to be not very short, satisfying the semiclassical condition (5) with δy instead of a. This leads to the condition $N \ll n$, where the number of magnetic flux quanta n is determined by Eq. (6). That condition does not contradict $1 \ll N$, since the number n is large.

The potential walls should not be infinitely steep. Otherwise, in the limit of $N\to\infty$ (perfectly rectangular potential barriers) the semiclassical approach is not valid. In the perfectly rectangular limit, the condition $|y_1|<\alpha$, resulting in Eq. (24), is substituted by $\mathrm{Re}\,y_1<\alpha$, which yields the condition $y^2<\alpha^2$. The consequence is that the reflection-induced curves in Fig. 1 degenerate into two lines $y=\pm\alpha$ and the underbarrier vortex state is not formed. The effect exists for any $N=1,2,\ldots$. in formula (4) [see also the discussion of the form of $u(y)$ in Ref. [7]]. We use a large N since it simplifies the solution of the Hamilton-Jacobi equation, allowing the reflectionless approach at some parts of the (x,y) plane.

IX. INTERPRETATION

The maxima of the electron density are shifted away from the line $y=0$ due to the disjoining effect near the vortex cores. An example of this distribution is shown in Fig. 3. The path $y=0$ provides a convenient indication of the resonance since along this path the effective potential (2) is real which allows interpretation in terms of the conventional Schrödinger equation (1).

The potential $U(x)$ can be calculated analytically in the case of a high magnetic field, $m\omega_c^2a^2 \gg |E|$, considered in Ref. [7], where $u(y)=u_0(y^2/a^2+y^4/a^4)$ was used. The decaying wave function is illustrated in Fig. 3. According to Eq. (1), apart from the vortex singularity, $x\neq 0$, the potential $U(x)$ can be written in the form

$$U(x) = \frac{\hbar^2}{2m|\psi(x,0)|}\frac{\partial^2|\psi(x,0)|}{\partial x^2} + E. \tag{36}$$

As follows from Fig. 3, at the extrema of $|\psi(x,0)|$ the function (36) is negative. In other words, the second term in Eq. (2) dominates. The derivative $\partial^2|\psi|/\partial y^2$ at $y=0$ is positive since the electron density is disjoined near the line $y=0$.

It is easy to calculate $U(x)$ on the basis of the results of Ref. [7]. Inside the barrier this potential has the form

$$U(x) = \frac{m\omega_c^2a^2}{4}\left[1+\sqrt{3}\tan\left(\frac{a(x-x_0)}{2l^2}\right)\right]. \tag{37}$$

The shift x_0 is chosen in order to get the singularities in the expression (37) at the vortex positions. The potential $U(x)$

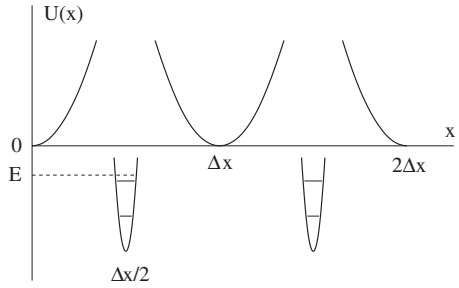

FIG. 4. Potential $U(x)$ close to the condition of Euclidean resonance. The parabolic semiclassical segments are connected in the vicinities of the points $\Delta x/2$ and $\Delta 3x/2$ by the nonsemiclassical wells of width $\delta \sim a/n \ll \Delta x \sim a$, which are shown schematically.

contains discrete energy levels of the order of $-m\omega_c^2 a^2$, which are smeared out to bands of the same order of magnitude. Since E is much smaller than that scale, it is not placed inside an allowed energy band. For this reason, the state is exponentially decaying.

The distribution of $|\psi(x,y)|$ in Fig. 3 corresponds to the limit $m\omega_c^2 a^2 \gg |E|$. As usual, it should be qualitatively similar at the border of applicability, $m\omega_c^2 a^2 \sim |E|$. In this limit, the topological vortex structure has to be of the same type as in Fig. 3, and the energy levels in the well $-m\omega_c^2 a^2$ are of the order of E. In this case energy coincidence is expected, which results in the resonance.

At the magnetic field $m\omega_c^2 a^2 \sim |E|$ the periodic potential $U(x)$ (2) can be evaluated from the results of Sec. V. At $\Delta x/2 < x < 3\Delta x/2$ the potential has the form $U(x) = m\omega_c^2 (x - \Delta x)^2/2$ shown in Fig. 4. These periodic parabolic segments are connected by potential wells located close to the points $\Delta x/2$ and $3\Delta x/2$ within the nonsemiclassical interval $\delta \sim l^2/a$ estimated in Sec. V. The total $U(x) \sim E$ is plotted schematically in Fig. 4. The discrete energy levels, shown in Fig. 4, are of the order of $-m\omega_c^2 a^2$ and slightly smeared out into narrow energy bands. Now one can expect a coincidence of the energy level $-m\omega_c^2 a^2$ with the electron energy $-E$, which is of the same order of magnitude. As we know from the calculations, it happens at $H = H_R$ (Euclidean resonance).

X. WHAT CAN BE OBSERVED IN EXPERIMENTS?

On the basis of the results of Sec. VI one can easily show that at $H < H_0$, where $H_0 \simeq 0.37 H_R$, the maximum of $|\psi(x,0)|$ is reached at $x=0$. At $H \simeq 0.16 H_0$ this situation is demonstrated in Fig. 5 where

$$P = \frac{\ln |\psi(x,0)|^2}{A_{WKB}(a)}. \tag{38}$$

In Fig. 5 only the semiclassical parts are shown, with empty spaces at the positions of vortices at the points $\Delta x/2$ and $3\Delta x/2$. The total horizontal interval is $2\Delta x$. The coordinate dependence in Fig. 5 is close to the case of zero magnetic field excepting small jumps at $\Delta x/2$ and $3\Delta x/2$. The jumps occur only in the semiclassical approximation used in Sec. V. The physical wave function is continuous. At higher magnetic field, $H_0 < H < H_R$, the maximum of $|\psi(x,0)|$ is reached at $x = \Delta x/2$. It is shown at $H \simeq 0.96 H_R$ in Fig. 6 where, as in Fig. 5, only the semiclassical parts are presented with empty spaces at the vortex positions. The total horizontal interval is also $2\Delta x$. In contrast to Fig. 5, there are strong oscillations of the wave function under the barrier. Close to the resonance field H_R, the amplitudes of the peaks decrease slowly in space according to a relation analogous to Eq. (33). Figure 6 corresponds to the schematic Fig. 2.

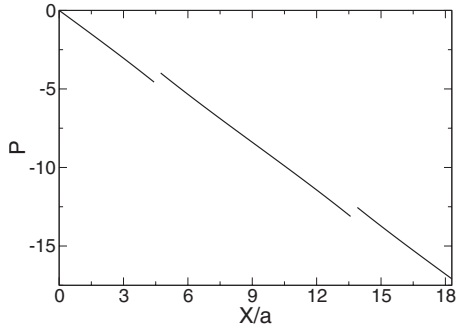

FIG. 5. Coordinate dependence of the logarithm of the wave function modulus at $H \simeq 0.16 H_0$. Only semiclassical parts are shown. We leave empty spaces at the vortex positions. The total horizontal interval is $2\Delta x$.

Looking at Figs. 5 and 6, one can draw conclusions about experimental observations of underbarrier phenomena in a magnetic field. Suppose, in a thin film, there is a quantum wire along the y axis with the discrete energy level $E \simeq -10^{-2}$ eV. Along the x axis there is a potential valley of the type (4) and of the width $a \simeq 200$ Å. At these parameters, $H_0 \simeq 10$ T and the wave function is localized under the barrier at the distance $x = \Delta x/2 \simeq 420$ Å apart from the quantum wire. This shift of the electron density far inside the barrier can be measured by a flat tunnel junction, which covers the region $x > 400$ Å, or some other technique. At a magnetic field much smaller than H_0 the electron density is localized at the wire and at the distance of 420 Å apart it is 10^{-19} compared to the wire region. The observable effect is caused by the threshold $(H > H_0)$ appearance of the underbarrier peak in the electron density.

One should note that instead of a potential of the type (4) one can take a positive potential, which is localized at the line $y=0$ (antiwire), for example, $u(y) = u_0 \exp(-y^2/a^2)$. In

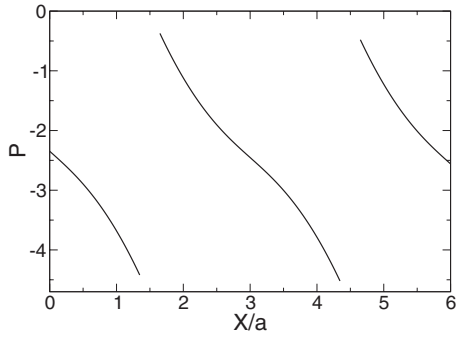

FIG. 6. As in Fig. 5 but at the field $H \simeq 0.96 H_R$.

this case the maxima of the wave function are localized at the line $y=0$ where the barrier is higher. Figures analogous to Figs. 5 and 6 look qualitatively the same. Proper calculations will be presented elsewhere with a discussion of more experimental details.

XI. DISCUSSION

We established an analogy between Euclidean resonance and conventional resonant Wigner tunneling by means of the effective potential $U(x)$, where a level coincides with the negative electron energy. It is clear that $U(x)$ should be negative at least in some regions. The necessary condition for this property, as follows from Eq. (2), is positivity of $\partial^2|\psi|/\partial y^2$ at some regions of x on the line $y=0$. In other words, the electron density should be disjoined at those regions. The disjoining effect is provided by the Lorentz force in the inner part of topological vortices, as noted in Sec. VII. So the logical chain of explanation of Euclidean resonance is the following: (1) creation of topological vortices; (2) disjoined electron density due to the Lorentz force produced by the vortex current; (3) a local positive $\partial^2|\psi|/\partial y^2$ as a result of the disjoined distribution; (4) an effective potential $U(x)$ with local negative potential wells; and (5) coincidence of a level in the well with the electron energy (Euclidean resonance as a form of resonant Wigner tunneling). In this sequence the transition from one item to another is logical. The last item provides the analogy we explore. The only unclear item is the initial one, creation of topological vortices. Actually, this question is the heart of the problem. Topological vortices under the barrier are created, for example, when $u(y)\sim y^4$, and are not created in the case of a quadratic $u(y)$. There is a mathematical way to understand this [the analytical properties of the function $u(y)$ in the complex plane] but it is impossible to propose general physical arguments to explain that difference. Indeed, why for some potential $u(y)$ the underbarrier state has a different topology? As a rule, physical arguments do not work for explanations of complicated interference. An example is the nonreflectivity of certain potentials due to interference of emitted partial de Broglie waves [1].

Euclidean resonance provides an example in condensed matter physics when the result is unexpected and cannot be predicted prior to calculations. Also, the dependence of topology on the form of the potential cannot be explained by hand-waving arguments.

Euclidean resonance means the formation of long-range coherence among effective potential wells, which is opposite to Anderson localization, when the coherence is destroyed [8]. One should note that Euclidean resonance is not only a property of a static potential barrier in a magnetic field, but also occurs in tunneling through nonstationary barriers [7,18–21]. In both cases an important issue is the formation of a phase of the wave function in the process of underbarrier motion. This leads to an interference of different underbarrier paths.

XII. CONCLUSION

In the process of conventional Wigner tunneling an electron encounters a classically allowed region, where the discrete energy level coincides with its energy. In our case the potential barrier is a constant in the direction of tunneling. But along the tunneling path certain regions are formed where, in the classical language, the kinetic energy of motion perpendicular to tunneling is negative. These regions play the role of potential wells, where a discrete energy level can coincide with the electron energy. This phenomenon, which occurs at a certain magnetic field, is called Euclidean resonance, and substantially depends on the shape of the potential forces in the direction perpendicular to tunneling. Under the conditions of Euclidean resonance, a long-distance underbarrier motion is possible, which can be experimentally observed. Euclidean resonance (formation of long-range coherence) constitutes a phenomenon that can be considered as the opposite pole with respect to Anderson localization (destruction of the long-range coherence).

ACKNOWLEDGMENTS

I am grateful to B. Shklovskii and A. Vainshtein for valuable discussions.

[1] L. D. Landau and E. M. Lifshitz, *Quantum Mechanics* (Pergamon, New York, 1977).
[2] B. I. Shklovskii, Pis'ma Zh. Eksp. Teor. Fiz. **36**, 43 (1982) [JETP Lett. **36**, 51 (1982)].
[3] B. I. Shklovskii and A. Efros, Zh. Eksp. Teor. Fiz. **84**, 811 (1983) [Sov. Phys. JETP **57**, 470 (1983)].
[4] V. Geshkenbein (unpublished).
[5] G. Blatter and V. Geshkenbein, in *The Physics of Superconductors*, edited by K. H. Bennemann and J. B. Ketterson (Springer-Verlag, Berlin, 2003).
[6] D. A. Gorokhov and G. Blatter, Phys. Rev. B **57**, 3586 (1998).
[7] B. I. Ivlev, Phys. Rev. A **73**, 052106 (2006).
[8] V. F. Gantmakher, *Electrons and Disorder in Solids* (Oxford University Press, Oxford, 2005).
[9] G. E. Volovik, Zh. Eksp. Teor. Fiz. Pis'ma Red. **15**, 116 (1972) [JETP Lett. **15**, 81 (1972)].
[10] A. V. Khaetskii and B. I. Shklovskii, Zh. Eksp. Teor. Fiz. **85**, 721 (1983) [Sov. Phys. JETP **58**, 421 (1983)].
[11] Q. Li and D. J. Thouless, Phys. Rev. B **40**, 9738 (1989).
[12] B. I. Shklovskii and B. Z. Spivak, in *Hopping Transport in Solids*, edited by M. Pollak and B. Shklovskii (North-Holland, Amsterdam, 1991).
[13] J. Hajdu, M. E. Raikh, and T. V. Shahbazyan, Phys. Rev. B **50**, 17625 (1994).
[14] M. E. Raikh and T. V. Shahbazyan, Phys. Rev. B **51**, 9682 (1994).
[15] L. D. Landau and E. M. Lifshitz, *Mechanics* (Pergamon, New York, 1977).
[16] J. Heading, *An Introduction to Phase-Integral Methods* (John Wiley, New York, and Methuen, London, 1962).

[17] P. G. de Gennes, *Superconductivity of Metals and Alloys* (Addison-Wesley, New York, 1989).
[18] B. I. Ivlev, Phys. Rev. A **66**, 012102 (2002).
[19] B. I. Ivlev and V. Gudkov, Phys. Rev. C **69**, 037602 (2004).
[20] B. I. Ivlev, Phys. Rev. A **70**, 032110 (2004).
[21] B. I. Ivlev, G. Pepe, R. Latempa, A. Barone, F. Barkov, J. Lisenfeld, and A. V. Ustinov, Phys. Rev. B **72**, 094507 (2005).